AIMS Mathematics

Research article

Image encryption with leveraging blockchain-based optimal deep learning for Secure Disease Detection and Classification in a smart healthcare environment

Fatma S. Alrayes[1], Latifah Almuqren[1], Abdullah Mohamed[2] and Mohammed Rizwanullah[3,*]

[1] Department of Information Systems, College of Computer and Information Sciences, Princess Nourah Bint Abdulrahman University, P.O. Box 84428, Riyadh 11671, Saudi Arabia
[2] Research Centre, Future University in Egypt, New Cairo, 11845, Egypt
[3] Department of Computer and Self Development, Preparatory Year Deanship, Prince Sattam bin Abdulaziz University, AlKharj, Saudi Arabia

* **Correspondence:** Email: r.mohammed@psau.edu.sa.

Abstract: Blockchain (BC) in healthcare can be used for sharing medical records and secure storage and other confidential data. Deep learning (DL) assists in disease recognition through image analysis, specifically in detecting medical conditions from images. Image encryption ensures the security and privacy of medical images by encrypting the image before sharing or storage. The combination of image encryption, BC, and DL provides an efficient and secure system for medical image analysis and disease detection in healthcare. Therefore, we designed a new BC with an Image Encryption-based Optimal DL for Secure Disease Detection and Classification (BIEODL-SDDC) technique. The presented BIEODL-SDDC technique enables the secure sharing of medical images via encryption and BC technology with a DL-based disease classification process. Furthermore, the medical image encryption process took place using the ElGamal Encryption technique with a giraffe kicking optimization (GKO) algorithm-based key generation process. In addition, BC-based smart contracts (SCs) were used for the secure sharing of medical images. For the disease detection process, the BIEODL-SDDC technique encompassed EfficientNet-B7-CBAM-based feature extraction, Adam optimizer, and a fully connected neural network (FCNN). The experimental validation of the BIEODL-SDDC technique was tested on medical image datasets and the outcome highlighted an enhanced accuracy outcome of 94.81% over other techniques.

1. Introduction

The smart healthcare system has received more attention with the development of the medical structure in recent times [1]. Smart healthcare denotes a set of rules that include treatment, prevention, management, and detection. Unlike conventional medical systems, smart medical systems can exchange and connect data anywhere and anytime [2]. Smart healthcare has the features of the interconnection of information, preventability, and immediacy of conventional medical treatment. With the wireless network, utilizing portable mobile gadgets, medical personnel can constantly analyze, perceive, and process major medical events (preventability). Clinicians can get the case data of all patients quickly and make a treatment plan and diagnosis (immediacy) [3]. Patients and other users log in to medical facilities through a healthcare information system, for retrieving health data through the internet. Secure communication was essential to ensure public network security and to protect patient privacy [4].

Information access, like healthcare, plays a major role in day-to-day lives because of rapid technological development [5]. Data sharing is becoming a hot research topic in personal healthcare. The security of data communication is more and more significant. For data management with other entities, this infrastructure necessitates secured data transmission [6]. Healthcare data is very private and data transmission may raise the exposure possibility. On top of that, the present method of data transmission uses a centralized structure that requires centralized trust. Encryption of delicate data is the vital and primary technique in cryptography regarding the historical data of patients [7]. Considering the digital health care technique as the environment for transferring and receiving medical data of patients. Transmitting medical data to authorized users becomes a crucial requirement of effective healthcare [8]. However, the current system lacks security methods as the majority of these cases lack suitable access control and encryption approaches. Many researchers have devised DL-based methods for disease detection [9]. Apart from that, DL methods necessitated higher computational resources and time to reach higher performance because of the complicated nature of the feature extraction process and image textures. Owing to the lack of availability of healthcare datasets [10], it is hard to take the true potential of DL methodology. A lot of training dataset is needed to use the actual potential of DL-related methods and realize an accurate and robust model.

We designed a new BC with an Image Encryption-based Optimal DL for Secure Disease Detection and Classification (BIEODL-SDDC) technique. In the presented BIEODL-SDDC technique, the medical image encryption process takes place using the ElGamal Encryption technique with a giraffe kicking optimization (GKO) algorithm-based key generation process. In addition, BC-based SCs are used for the secure sharing of medical images. For the disease detection process, the BIEODL-SDDC technique encompasses EfficientNet-B7-CBAM-based feature extraction, Adam optimizer, and a fully connected neural network (FCNN). The experimental validation of the BIEODL-SDDC method is tested on medical image datasets.

The remaining sections of the article are arranged as: Section 2 offers literature review, and section 3 represents the proposed method. Then, section 4 elaborates on the results evaluation, and section 5 completes the work.

2. Related works

The researchers in [11] presented an innovative hybrid Deep Belief-based Diffie Hellman (DBDH) security structure for the protection of healthcare data against malicious events. Through the incorporation of a DBN mechanism constantly oversee the mechanism and find the attacks. Initially, from the standard site, the IoMT dataset has been collected and imported into the mechanism. Also, hash 1 has been computed for the original database and saved in the cloud server for authentication. Then, for data hiding, the original dataset was encoded with private keys. The amalgamation of homomorphic properties will be helpful in the computation of hash 2 for the encoded dataset. Jadav et al. [12] offer a BC and AI-envisioned secure and trusted framework (HEART). In this study, to classify wearable devices as non-malicious or malicious, LSTM was employed. Next, the researcher devises an SC that permits only the patient dataset with wearable devices that should be categorized as non-malicious to public BC networks. This data can be accessed by those who are indulged in the patient's care.

Pustokhina et al. [13] introduced a novel BC-based secured data-sharing scheme (BBSDSS) with the use of image encryption and steganography approaches for telemedicine applications. This particular method has 3 stage processes they are encryption, secure data sharing, and image steganography. The glowworm swarm optimization method was implemented first for the image steganography procedure. This method involved a signcryption system to encode the stegno images. Later the BC method can be implemented to enable the safe sharing of patient records. Wu et al. [14] devised a new content-aware deoxyribonucleic acid (DNA) computing mechanism to encode healthcare images, consequently promoting a secure healthcare environment and guaranteeing privacy. This system contains a receiver and sender to execute tasks of decryption and encryption, which comprise a similar structure but effectuate opposite operations. In receiver or sender, the author designed an arbitrary DNA encoding and content-aware permutations and diffusion modules.

Noman et al. [15] devised a federated learning (FL) system that learns from multiclass and heterogeneous respiratory healthcare datasets. This system aggregates and trains local methods using BC technology. The weight manipulation approach is also presented dissimilar to other studies while aggregating the local methods, which employ local model test accurateness as principal parameters. Ren et al. [16] devised a BC-driven tensor meta-learning-powered intellectual healthcare system with IoT assistance. IoT gadgets such as light nodes upload local shared datasets to full nodes for training the model and effectuate local private datasets by a non-tampered method downloaded through an SC. To be specific, a tensor meta-learning algorithm termed tensor-prototype graph network was formulated. Singh et al. [17] integrated Fog computing and AI including smart health for carrying out reliable platforms for initial-stage identification of COVID-19. An innovative ensemble-based technique was devised for diagnosing COVID-19 patients. The researchers also provided a BC technology.

Ala et al. [18] introduced a new model within smart healthcare systems (SHS) by incorporating artificial intelligence (AI) and the Internet of Things (IoT). The approach also presented the integration of the Particle Swarm Optimization-Long Short-Term Memory (PSO-LSTM) technique into the IoT-based SHS model for optimization purposes. In [19], the authors concentrated on establishing a Smart Deals System (SDS), leveraging improved machine learning (ML) models. Furthermore, a secure consumer application is also designed, which is centered around human requirements for facilitating the system's functionality. Ala et al. [20] proposed a Mixed-Integer Linear Programming (MILP) approach. The objective of the Admission Scheduling Problem (ASP) model is to reduce patient waiting time. We

also explored the Fuzzy Ant Lion Optimization (FALO) strategy and Non-dominated Sorting Genetic Algorithm II (NSGA-II) approaches for addressing the multi-objective ASP.

3. The proposed model

In this study, a BIEODL-SDDC technique is developed for a secure and smart healthcare environment. The presented BIEODL-SDDC technique allows the secure sharing of medical images via encryption and BC technology with a DL-based disease classification process. It involves three major processes: Image encryption, secure data distribution, and disease diagnosis module. Figure 1 depicts the workflow of the BIEODL-SDDC algorithm.
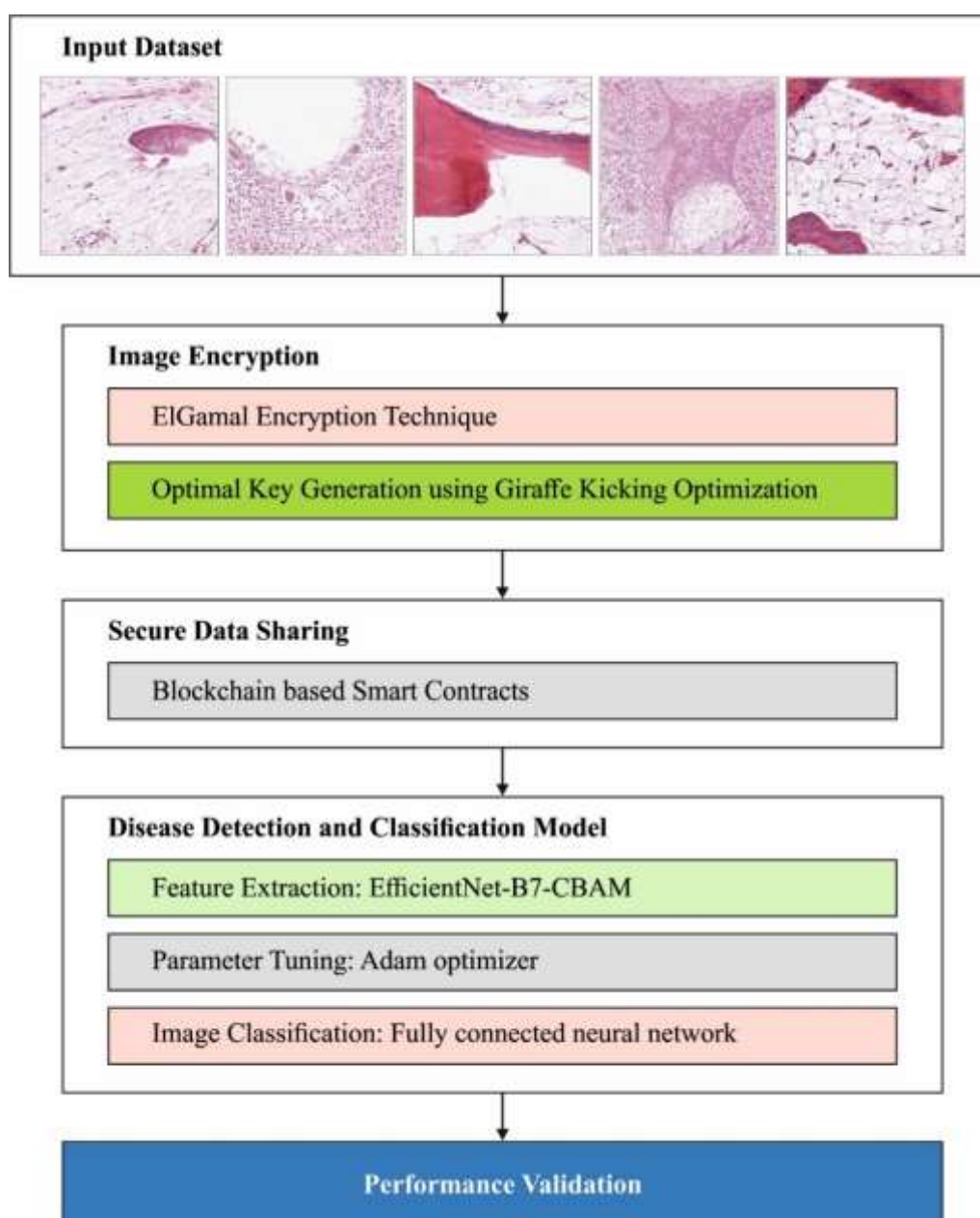

Figure 1. Workflow of BIEODL-SDDC algorithm.

3.1. ElGamal encryption with optimal key generation

At the initial stage, the medical image encryption process is performed by the ElGamal Encryption technique. The ECC-based ElGamal encryption using various steps and parameters is shown below [21]. The additive homomorphic method can be formulated using the following equation,

$$E(m_1) + E(m_2) = E(m_1 + m_2) \tag{1}$$

where the "+" symbol is projected for the additive homomorphic and the public key is represented as "E". The additive homomorphic encryption can be assumed in ECC. Based on the elliptic curve's (ECs) algebraic infrastructure on finite domains, ECC-based ElGamal is illustrated. The finite field was divided into 2 types, namely binary and prime fields 2_n. In this analysis, ECs over the prime field were inspected. The special class of EC illustrated in Eq (2) used in EC over real numbers as follows,

$$y^2 = x^3 + ax + b \tag{2}$$

In Eq (2), $E_r(a, b)$ represents the resulting curve where the modulus is r, and a and b represent the new coefficients. The x value ranges from zero to r and is on the curve. Also, using lower bit size ECC projected related security level by processing overhead decreases when we compare with homomorphic and RSA approaches.

To optimally choose the keys involved in the ElGamal Encryption algorithm, the GKO algorithm is used. The GKO is a novel metaheuristic algorithm, motivated by the kicking behaviour of giraffes [22]. The mother giraffe starts to bond with her calf and lick it clean of residual amniotic fluid. Similarly, they urge the calf to remain by commonly kicking 3 times and making the first stride that enables the youthful giraffe to nurture originally and this can be performed in real-time solicitations such as optimized data clustering, and information routing. The mathematical expression is formulated by the 3 times kicking style of the giraffe and the formula is defined in the following that assists in making the sensor energetic from sleeping mode and provides better performance and fast data transmission.

$$\overrightarrow{Dl_\alpha} = \left| \vec{F} \cdot \overrightarrow{KP}(ti) - \vec{K}(ti) \right| \tag{3}$$

$$\vec{K}(ti + 1) = \overrightarrow{KP}(t) - \vec{W} \cdot \overrightarrow{Dl_\alpha} \tag{4}$$

where ti denotes the existing location, $\vec{W}$ and $\vec{F}$ indicate the Coefficient vector, $\overrightarrow{KP}$ represents the location vector of the infant, and $\vec{K}$ indicates the location vector of the Giraffe as defined below:

$$\vec{W} = 5 \cdot \vec{\alpha} \cdot \overrightarrow{r1} - \vec{\alpha} \tag{5}$$

$$\vec{F} = 5 \cdot \overrightarrow{r2} \tag{6}$$

$$\vec{\alpha} = 5 - \left(iteration_{algo} \times \frac{5}{\text{Max}_{iteration}} \right) \tag{7}$$

where $iteration_{algo} = 1, 2, \ldots, \text{Max}_{iteration}$.

Let $\vec{\alpha}$ be the random number within [0,5] for making the balance between the exploration and exploitation of the maximal amount of iteration, and $r1$ and $r2$ were random vectors within [0,1]. From the abovementioned condition, a giraffe in the condition of (K, Y) could invigorate its situation according to the infant situation (K^*, Y^*). $\overrightarrow{Dl_\alpha}$ is represented as the space amongst the infant and mother giraffes and ti denotes the existing location of the giraffe. This method encourages further exploitation according to the iteration values increasing quickly. For instance, $(K^* - K, Y^*)$ set as $\vec{\alpha} = (1,0)$ and

$\vec{F} = (1,1)$. The random vectors help the giraffe to obtain any state amongst two certain points. Hence, a giraffe could rejuvenate its location intimate space toward the infant in a random zone as follows.

$$\overrightarrow{Dl}\alpha = \left| \overrightarrow{F1} \cdot \overrightarrow{K\alpha} - \vec{K} \right| \tag{8}$$

$$\overrightarrow{Dl}\beta = \left| \overrightarrow{F1} \cdot \overrightarrow{K\beta} - \vec{K} \right| \tag{9}$$

$$\overrightarrow{Dl}\delta = \left| \overrightarrow{F1} \cdot \overrightarrow{K\delta} - \vec{K} \right| \tag{10}$$

$$\vec{K}1 = \overrightarrow{K\alpha} - \overrightarrow{W}1 \cdot \left(\overrightarrow{Dl}\alpha \right) \tag{11}$$

$$\vec{K}2 = \overrightarrow{K\beta} - \overrightarrow{W}1 \cdot \left(\overrightarrow{Dl}\beta \right) \tag{12}$$

$$\vec{K}3 = \overrightarrow{K\delta} - \overrightarrow{W}1 \cdot \left(\overrightarrow{Dl}\delta \right) \tag{13}$$

$$\vec{K}(ti + 1) = \frac{\vec{K}1 + \vec{K}2 + \vec{K}3}{3} \tag{14}$$

From the expression, a pursuit expert rejuvenates its condition in n-dimensional inquiry space. Furthermore, the end location could be in an unbalanced spot inside the territory that can be classified by the condition of the giraffe during hunt space. Figure 2 defines the flowchart of GKO.
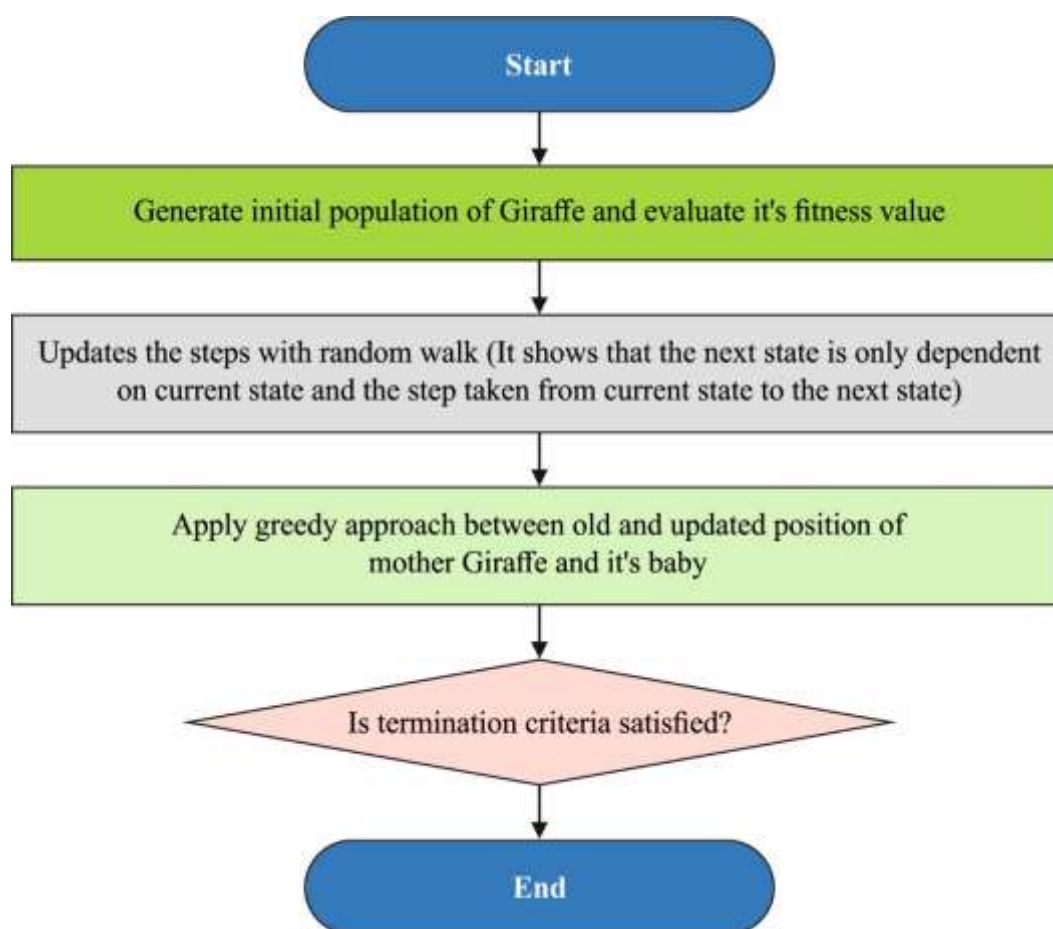

Figure 2. Flowchart of GKO.

Exploitation provides converged or better results. The vacillation selection of $W \rightarrow$ is further decreased by $\rightarrow_\alpha$. $W \rightarrow [0,1]$ represents an unequal enticement within the interval $[-5a, 5a]$. a was reduced from 5 to 0. The process is prone to stagnate in adjacent arrangements with this administrator.

Exploration explores or gets better rewards. They deviate from each other to find the child and kick the infant giraffe. $\vec{W}$ is a random quality greater than 1 to assist the search expert in finding the infant giraffe. This enables the algorithm and underlines investigation to look all-around $|W|$ shows the mother giraffe to be removed from the child to ideally find a better arrangement. An additional role of calculation that favors analysis is $\vec{F}$ which has random quality within $[0, 2]$. This part provides a random load to the child giraffe for de-accentuate $(F < 1)$ or stochastically stress $(F > 1)$ the influence of the child in describing the separation. The $'F'$ is considered as an effect of difficulties in moving towards a child giraffe. Each applicant arrangement rejuvenates the separation from the child giraffe. In general, hopeful arrangements deviate from the infant giraffe if $|\vec{W}| > 1$ and bond toward the child if $|\vec{W}| > 1$.

For the maximization of PSNR value, the GKO technique derives a fitness function in this study.

$$Fitness = max\ (PSNR) \tag{15}$$

3.2. BC-based secure data sharing

The SC allows privacy and security to share information among the clinics [23]. The SC is applied for a secured sharing of data to allow the uploading of the medical image automatically. According to the terms and conditions related to the data-sharing agreement, it generates the parameter. An SC allows access for exchanging the image dataset amongst the clinics. The IPFS stores the local model weight with reference id (hashes) in the BC database. Authorized or registered hospitals share the locally trained DL model's weight via SC. An SC allows a sharing model on the BC. Moreover, the BC network has multiple parties and a fully distributed data collection framework, a registered organization is only allowed to access the data. The SC ensures the reliability and transparency of the BC across geographically distributed nodes. The idea has been revitalized and the design of SC has been facilitated.

The organization registers its information with the RegisterData function. For fetching the information, the address, hash, price, and description features are used. Afterwards uploading the information in the BC, each hospital access information with the authorization of another organization. The access token allows data sharing. Organizations share a sequence of healthcare datasets, and only an authorized client accesses the information. The ownership of data and the owner of Register Hospitals (H) are responsible for a digital signature on data. In the BC ledger, the tokens are generated. The SC assurances that the shared image comes from the authorized source. The SC uploads the information in the BC with the signature of the registered hospital. Moreover, it assists in providing decision support and more accurate predictions for security concerns.

Every hospital shares the local model's weight and downloads the updated weight for the collectively constructed model. The hospital locally computes the gradient and transmits the weight to the global BC. The BC calculates the node and aggregates the model. The SC shares the aggregated outcomes with the hospital without disclosing the original data of the images. Furthermore, the input of local model weight is passed over to the BC decentralized system, and the updated model output can be shared in the decentralized system, after processing the input. Thus, collecting each new case of disease detection via the SC to train a collaborative DL method is an efficient way.

3.3. DL-based disease detection

For the disease detection process, the BIEODL-SDDC technique encompasses EfficientNet-B7-CBAM-based feature extraction, Adam optimizer, and FCNN.

3.3.1.   Feature extraction: EfficientNet-B7-CBAM

At this stage, the EfficientNet-B7-CBAM architecture is applied to produce feature vectors. The advent of EfficientNet is based on the balance between width, resolution, and depth [24]. B0-B7 EfficientNet is a new version of EfficientNet-B7-CBAM. The basic framework of the network was Mobile Inverted Bottleneck Convolution (MBConv). This model presents the core concept of the Squeeze-and-Excitation (SE) model to enhance the Network structure. First, the MBConv uses 1x1 convolution to up-dimension the feature maps, and afterward kxk depthwise convolution. Next, the SE module adjusts the feature map matrix, and finally, 1x1 convolution to down-dimension the feature maps. Also, the MBConv can able to perform short-cut concatenation once the input and output feature mappings have a similar shape. This decreases the training time. A conventional Efficientnet-B7 comprises 1 layer of FC classification, 55 layers of MBConv module, 2 layers of Conv module, and 1 layer of global average pool. EfficientNetB7 is encompassed by the stacked MBConv, with every MBConv model having a SE model. The SE model controls the gating or focus of the channel dimension. The module emphasizes channel features that have the majority of data while disregarding the trivial channel features. However, this process considered the data of the channel and lost the spatial data, which plays a vital role in visual recognition that adversely affected the classification accuracy. In this study, add a CBAM to Efficientnet-B7 to optimize the ability of the model to feature extraction.

The SE model in every MBConv of the original EfficientNetB7 architecture was replaced by a CBAM model. This allows obtaining channel data without the loss of spatial data concerning pepper plug seedlings. After the second Conv layer, the CBAM model was embedded in the EfficientNet-B7-CBAM module. It improves the ability of the module to categorize dissimilar quality plug seedlings by improving the classification ability and refining the extracted feature data.

In addition, the Adam optimizer is used for the hyperparameter tuning process. It is an optimization technique, as an alternative to the SGD method for the network weight updating during the training dataset [25], and implements optimization and it is one of the better optimizers. Adam is an adaptable technique based on Adagrad where ADAGRAD and momentum are together termed Adam. Parameters $w^{(t)}$ and $L^{(t)}$, where index t shows the existing training iteration, Parameter updating in ADAM can be represented as follows:

$$m_w^{(t+1)} \leftarrow \beta_1 m_w^{(t)} + (1 - \beta_1)\nabla_w L^{(t)} \tag{16}$$

$$v_w^{(t+1)} \leftarrow \beta_2 v_w^{(t)} + (1 - \beta_2)(\nabla_w L^{(t)})^2 \tag{17}$$

$$\widehat{m}_w = \frac{m_w^{(t+1)}}{1 - (\beta_1)^{(t+1)}} \tag{18}$$

$$V_w = \frac{v_w^{(t+1)}}{1 - (\beta_2)^{(t+1)}} \tag{19}$$

$$w^{t+1} \leftarrow w^t - \eta \frac{\widehat{m}}{\sqrt{\widehat{v}_w} + \epsilon} \tag{20}$$

where β_1 and β_2 indicate the gradient forgetting factor and 2nd moment of the gradient. In Eq. (20), $\in$ denotes the small scalar used for avoiding division by 0.

3.3.2.   Image classification: FCNN Model

The FCNN is the popular DL network [26], where every node in the FC layer is interconnected to all the nodes of the succeeding layer, and every connection has a correspondingly specific and different weight that is not shared by any node. To classify the medical images, the generated features are examined by the FCNN model. The FCNN is better than RNN and CNN, it is known that the performance degradation was caused by the gradient disappearing problems during backpropagation. Though the backpropagation problem had constrained the development of ANN, it was solved by the advent of the ReLU function.

Therefore, most DL technique use the ReLU function to prevent the gradient disappearing problem using the sigmoid function. Also, leaky ReLu is adopted as an activation function, like RELU. At the last layer, the $softmax$ function with cross-entropy cost function generates the last outcome for every input dataset. The common formula for softmax activation function, Leaky ReLU, sigmoid, and ReLu are given below:

$$Sigmoid \ = \frac{1}{1+e^{-x}} \tag{21}$$

$$ReLU = \begin{cases} 0 \ for \ x < 0 \\ x \ for \ x \geq 0 \end{cases} \tag{22}$$

$$LeakyReLU \ = \begin{cases} 0.01x & for x < 0 \\ x & for \ x \geq 0 \end{cases} \tag{23}$$

$$Softmax \ (x_i) = \frac{e^{x_i}}{\sum_{j=1}^{n} e^{x_j}} \tag{24}$$

In the final layer, the three-layer MLP with softmax function is similar to the multi-class logistic regression method. Generally, MLP with n hidden layers are mathematically expressed in the following:

$$H(x) = H_n(H_{n-1}(H_{n-2}(\cdots (H_{1(x)}))))) \tag{25}$$

The activation function, the number of hidden layers, and the output class are the parameters for constructing NNs to dynamically configure in the platform. At the output layer, the $softmax$ function with the cross-entropy cost function generates the final output.

4.   Results and discussion

The experimental validation of the BIEODL-SDDC technique is tested on the osteosarcoma dataset [27], covering 1144 images under three classes as provided in Table 1. It includes 345 images under viable tumor (VT), 536 images under Non-Tumor (NT), and 263 images under the non-viable Tumor (NVT) class. The suggested technique is simulated by utilizing the Python 3.6.5 tool on PC i5-8600k, 250GB SSD, GeForce 1050Ti 4GB, 16GB RAM, and 1TB HDD. The parameters settings are provided as: learning rate: 0.01, activation: ReLU, epoch count: 50, dropout: 0.5, and size of the batch: 5.

Figure 3 shows the histogram analysis of the BIEODL-SDDC technique. Figure 3a demonstrates the original images and its histogram representation is provided in Figure 3b. Then, the encrypted image by the

BIEODL-SDDC technique is depicted in Figure 3c and the respective histograms are given in Figure 3d.

Table 1. Details of database.

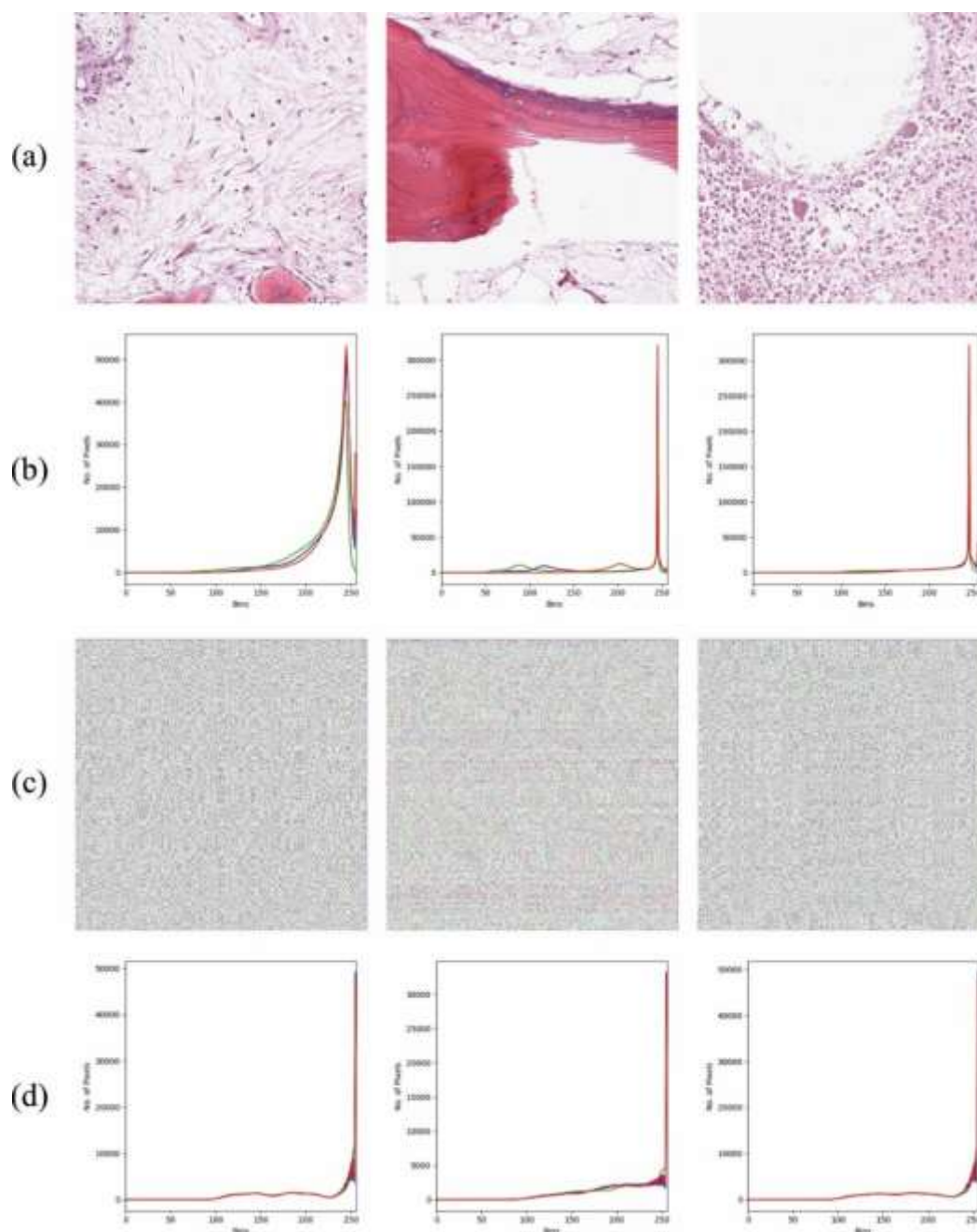| Class	No. of Samples
Non-Tumor	355
Non-Viable Tumor	263
Viable Tumor	536
Total Number of Samples	**1154**

Figurte 3. a) Original Images, b) Histogram of Original Images, c) Encrypted Images, and d) Histogram of Encrypted Images.

The MSE examination of the BIEODL-SDDC technique is studied with existing ones in Table 2 and Figure 4. The figure exhibits the CO-ECC method results in poor performance with exceeding MSE values. Then, the hybrid-CE and PSOECC models obtain moderately reduced MSE values. Then, the BEEPO and BPPIE models reached considerable MSE values. However, the BIEODL-SDDC technique outperforms the other models with minimal MSE of 0.082, 0.053, 0.123, 0.156, and 0.151, respectively.

Table 2. MSE analysis of BIEODL-SDDC approach with other systems on several images**.**

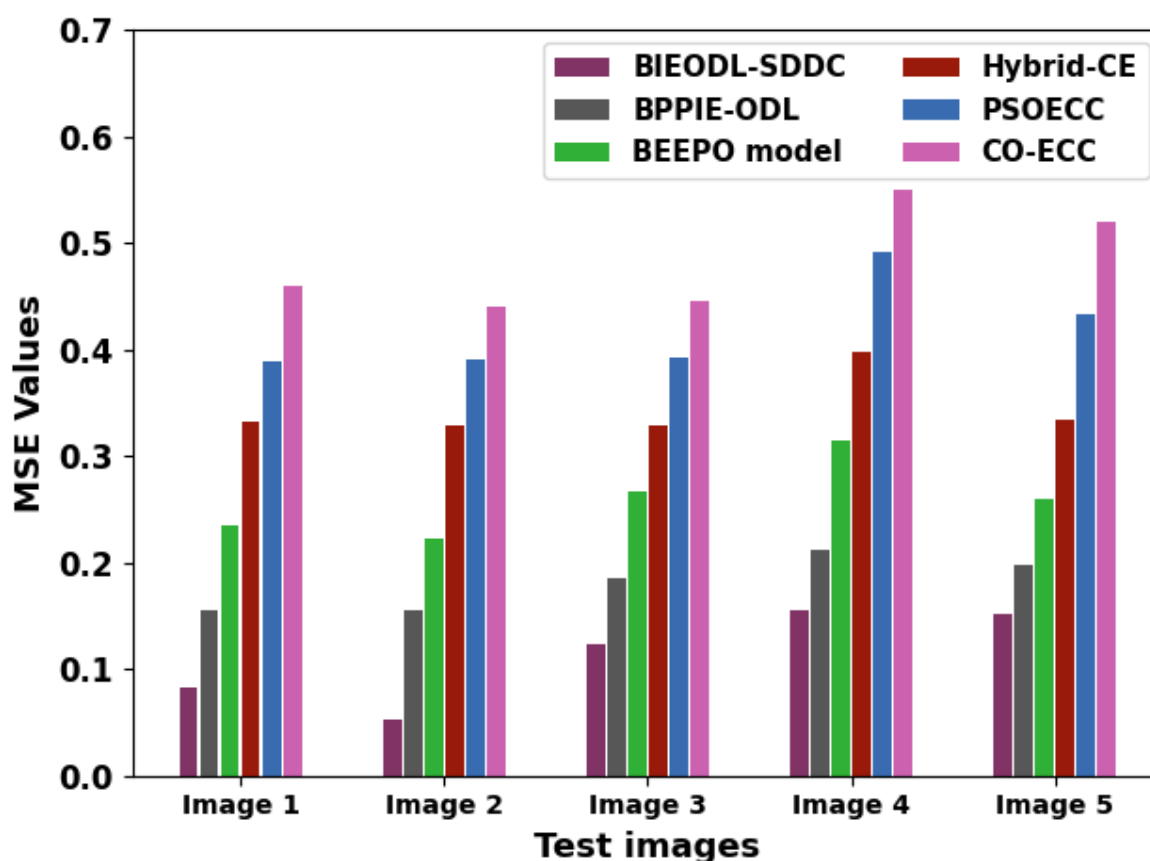| MSE Values						
Test images	BIEODL-SDDC	BPPIE-ODL	BEEPO model	Hybrid-CE	PSOECC	CO-ECC
Image 1	0.082	0.156	0.235	0.332	0.389	0.459
Image 2	0.053	0.156	0.223	0.329	0.391	0.440
Image 3	0.123	0.186	0.267	0.329	0.392	0.445
Image 4	0.156	0.211	0.314	0.398	0.491	0.549
Image 5	0.151	0.198	0.260	0.333	0.433	0.519

Figure 4. MSE analysis of the BIEODL-SDDC approach on several images.

The PSNR examination of the BIEODL-SDDC technique is studied with existing ones in Table 3 and Figure 5. The outcomes display that the CO-ECC method results in poor performance with the

least PSNR values. Then, the hybrid-CE and PSOECC models obtain moderately improved PSNR values. Then, the BEEPO and BPPIE models reached considerable PSNR values. However, the BIEODL-SDDC technique outperforms the other models with higher PSNR of 58.99dB, 60.89dB, 57.23dB, 56.20dB, and 56.34dB, respectively.

Table 3. PSNR analysis of BIEODL-SDDC approach with other systems on several images.

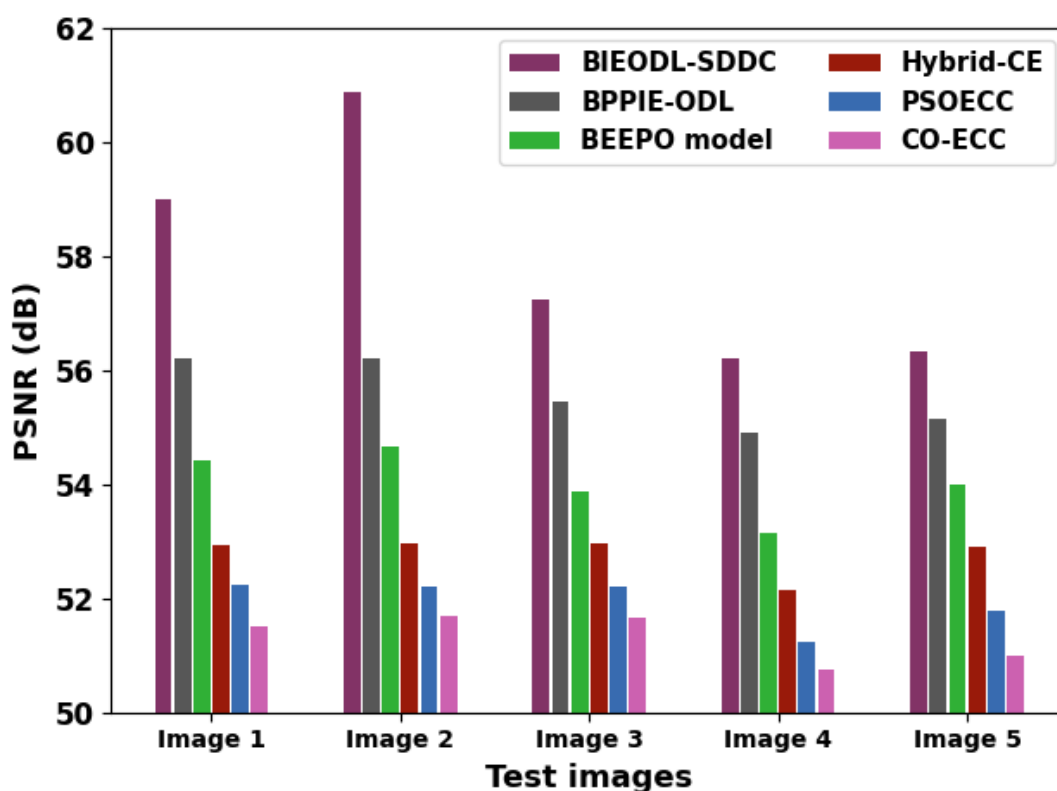| PSNR (dB)						
Test images	BIEODL-SDDC	BPPIE-ODL	BEEPO model	Hybrid-CE	PSOECC	CO-ECC
Image 1	58.99	56.20	54.42	52.92	52.23	51.51
Image 2	60.89	56.20	54.65	52.96	52.21	51.70
Image 3	57.23	55.44	53.87	52.96	52.20	51.65
Image 4	56.20	54.89	53.16	52.13	51.22	50.74
Image 5	56.34	55.16	53.98	52.91	51.77	50.98

Figure 5. PSNR analysis of BIEODL-SDDC approach on several images.

The CC examination of the BIEODL-SDDC technique is studied with existing ones in Table 4 and Figure 6. The figure indicates that the CO-ECC method results in poor performance with the least CC values. Then, the hybrid-CE and PSOECC models obtain moderately improved CC values. Thereafter, the BEEPO and BPPIE models reached considerable CC values. However, the BIEODL-SDDC technique outperforms the other models with higher CC of 99.40%, 99.56%, 99.74%, 99.96%, and 99.75%, respectively.

Table 4. CC analysis of the BIEODL-SDDC approach with other systems on several images.

Correlation Co-efficient (%)						
Test images	BIEODL-SDDC	BPPIE-ODL	BEEPO model	Hybrid-CE	PSOECC	CO-ECC
Image 1	99.40	99.04	99.06	98.83	98.53	98.45
Image 2	99.56	99.22	99.11	99.00	98.82	98.30
Image 3	99.74	99.28	99.09	99.10	98.73	98.35
Image 4	99.96	99.46	99.44	98.99	98.91	98.51
Image 5	99.75	99.38	99.15	99.11	98.62	98.70
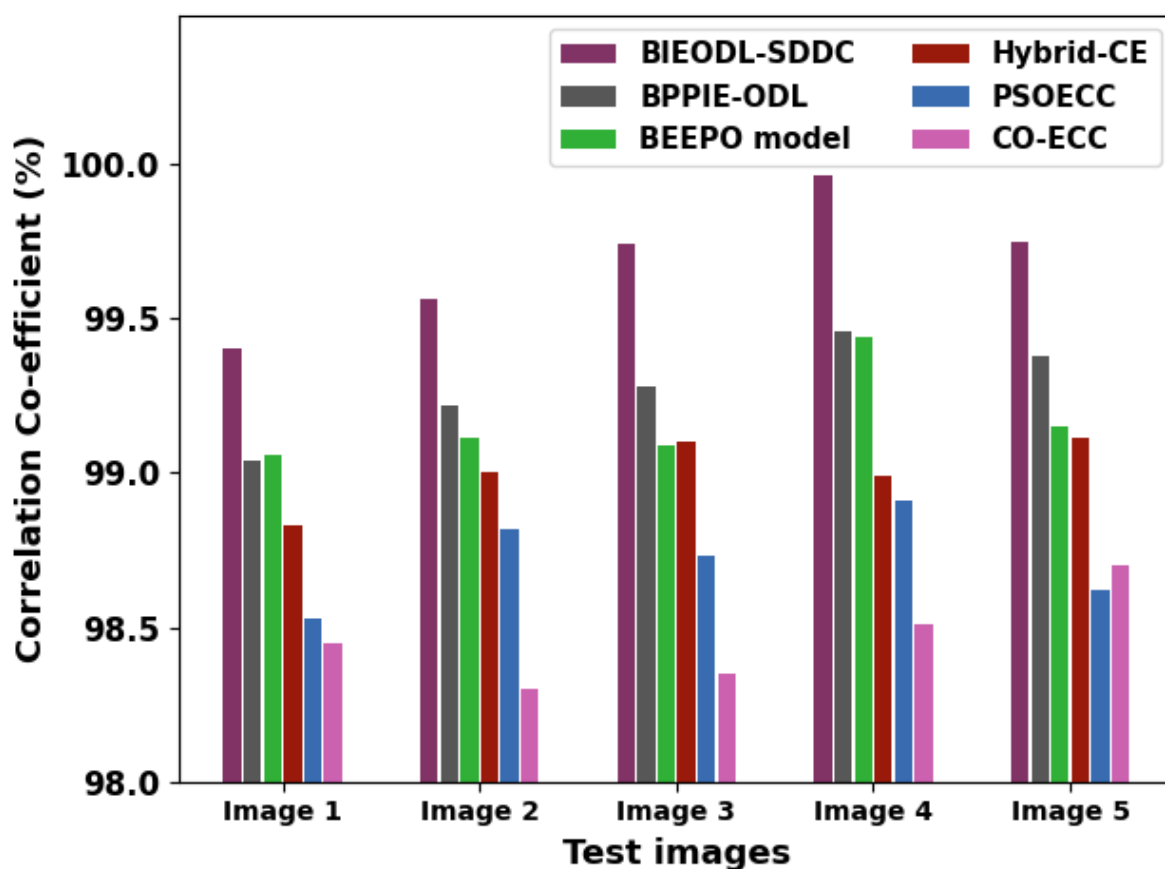
Figure 6. CC analysis of BIEODL-SDDC approach on several images.

The CT examination of the BIEODL-SDDC technique is studied with existing ones in Table 5 and Figure 7. The outcomes indicate that the CO-ECC approach results in poor performance with exceeding CT values. Then, the hybrid-CE and PSOECC models obtain moderately reduced CT values. Thereafter, the BEEPO and BPPIE models reached considerable CT values. However, the BIEODL-SDDC technique outperforms the other models with minimal CT of 38.23s, 33.21s, 30.11s, 46.87s, and 37.68s, respectively.

Table 5. CT analysis of the BIEODL-SDDC approach with other systems on several images.

Computational Time (sec)						
Test images	BIEODL-SDDC	BPPIE-ODL	BEEPO model	Hybrid-CE	PSOECC	CO-ECC
Image 1	38.23	42.59	54.91	65.35	101.02	110.91
Image 2	33.21	36.26	40.68	57.74	116.55	120.56
Image 3	30.11	32.34	39.9	41.29	127.62	146.76
Image 4	46.87	50.42	62.61	77.25	138.34	148.87
Image 5	37.68	41.79	48.44	59.17	129.46	155.15
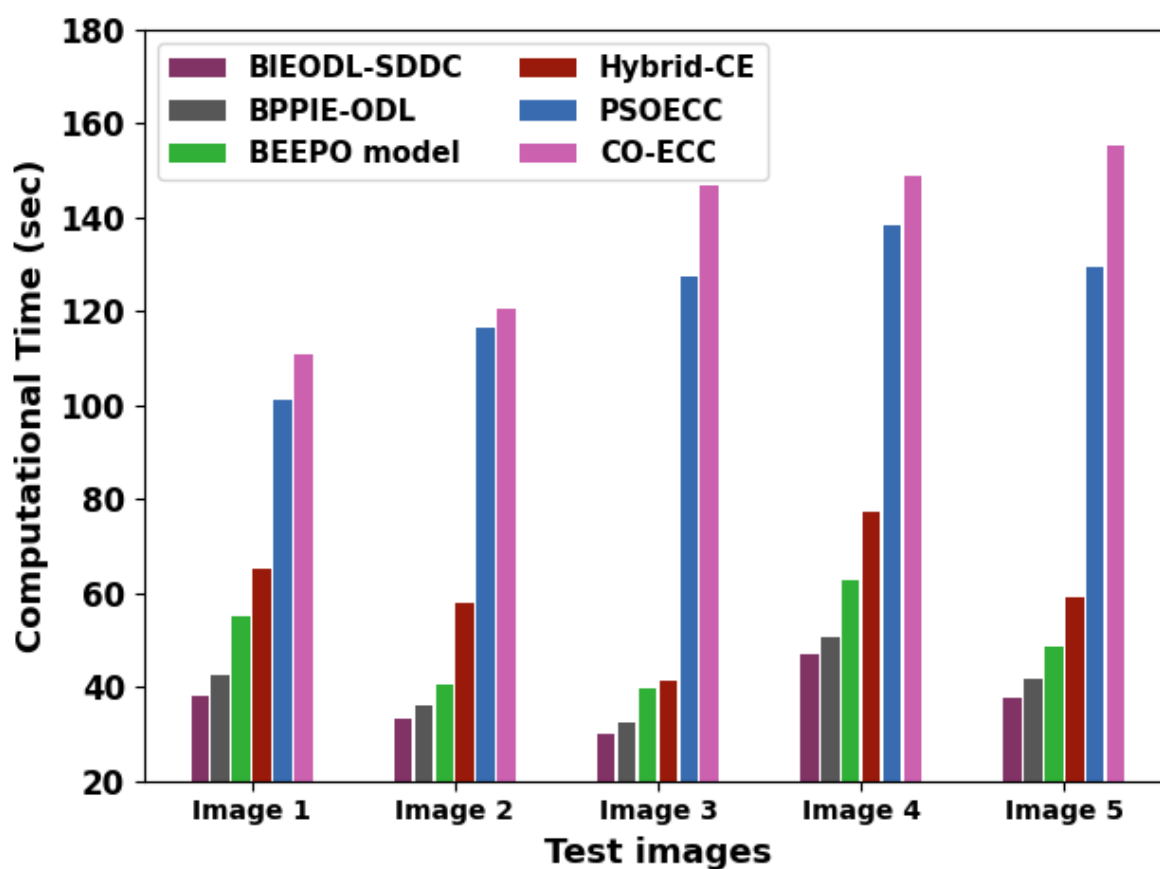
Figure 7. CT analysis of the BIEODL-SDDC approach on several images.

The confusion matrices of the BIEODL-SDDC technique are exhibited in Figure 8. The outcomes exhibit that the BIEODL-SDDC technique reaches proficient performance in the osteosarcoma classification process.
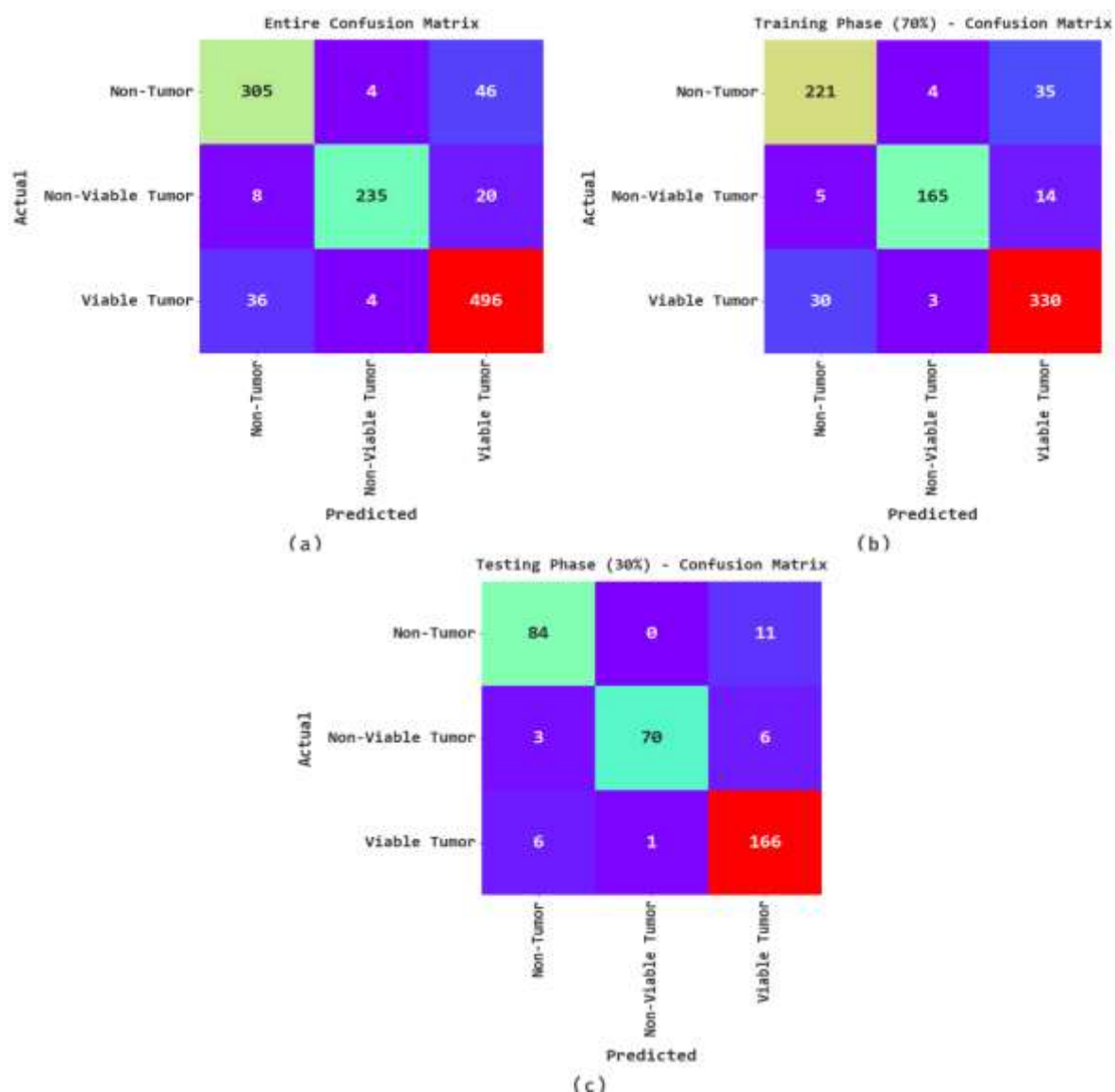
Figure 8. Confusion matrices of BIEODL-SDDC algorithm (a) Entire, (b) 70% of TRP, and (c) 30% of TSP.

The classifier outcomes of the BIEODL-SDDC technique are deliberated in Table 6. The outcomes indicate that the BIEODL-SDDC technique recognized all kinds of tumors. For the dataset, the BIEODL-SDDC technique attains an average $accu_y$ of 93.18%, $prec_n$ of 90.79%, $reca_l$ of 89.27%, F_{score} of 89.96%, and $Jaccard_{index}$ of 81.85%. Moreover, for 70% of TRP, the BIEODL-SDDC technique attained an average $accu_y$ of 92.48%, $prec_n$ of 89.78%, $reca_l$ of 88.53%, F_{score} of 89.10%, and $Jaccard_{index}$ of 80.47%. Eventually, for 30% of TSP, the BIEODL-SDDC technique attained an average $accu_y$ of 94.18%, $prec_n$ of 93.21%, $reca_l$ of 90.99%, F_{score} of 91.98%, and $Jaccard_{index}$ of 85.21%.

The TACY and VACY of the BIEODL-SDDC technique are inspected on BC performance in Figure 9. The figure highlighted that the BIEODL-SDDC approach has improvised performance with higher values of TACY and VACY. The BIEODL-SDDC technique has greater TACY outcomes.

Table 6. Classifier outcome of BIEODL-SDDC approach with various classes.

Class	Accuracy	Precision	Recall	F-Score	Jaccard Index
Entire Dataset					
Non-Tumor	91.85	87.39	85.92	86.65	76.44
Non-Viable Tumor	96.88	96.71	89.35	92.89	86.72
Viable Tumor	90.81	88.26	92.54	90.35	82.39
Average	**93.18**	**90.79**	**89.27**	**89.96**	**81.85**
Training Phase (70%)					
Non-Tumor	90.83	86.33	85.00	85.66	74.92
Non-Viable Tumor	96.78	95.93	89.67	92.70	86.39
Viable Tumor	89.84	87.07	90.91	88.95	80.10
Average	**92.48**	**89.78**	**88.53**	**89.10**	**80.47**
Testing Phase (30%)					
Non-Tumor	94.24	90.32	88.42	89.36	80.77
Non-Viable Tumor	97.12	98.59	88.61	93.33	87.50
Viable Tumor	93.08	90.71	95.95	93.26	87.37
Average	**94.81**	**93.21**	**90.99**	**91.98**	**85.21**
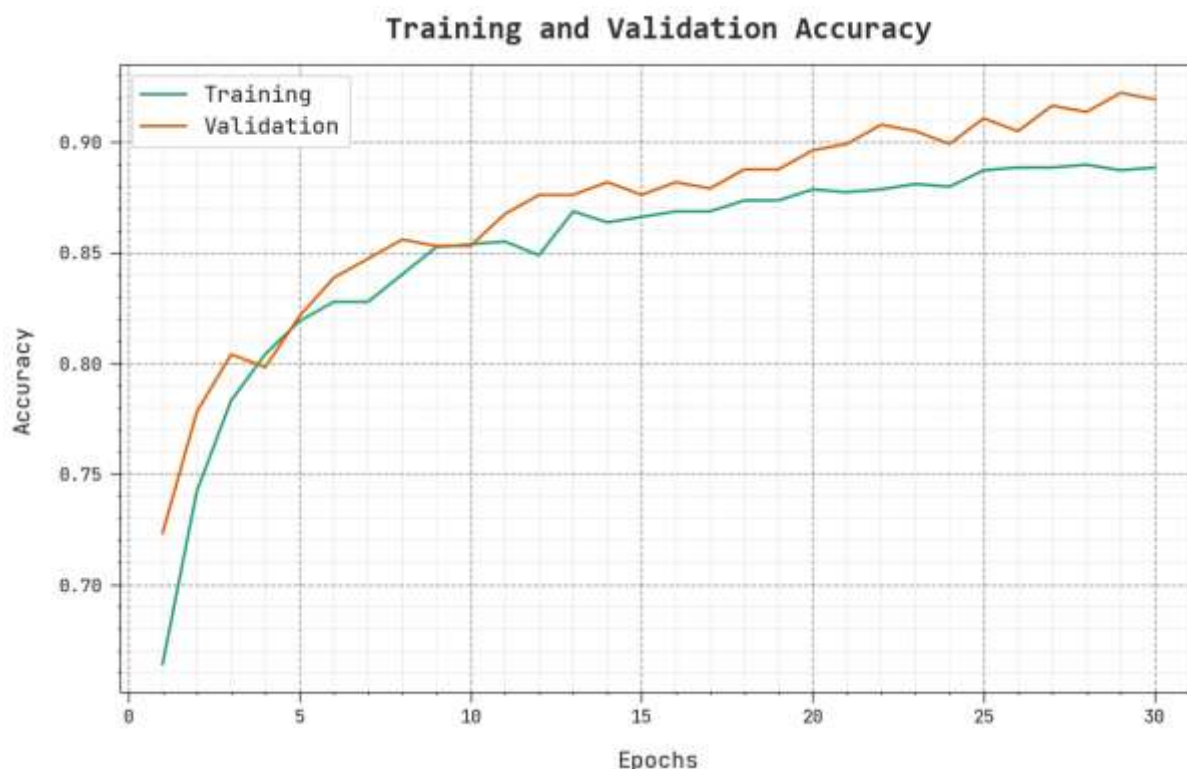
Figure 9. TACY and VACY outcomes of the BIEODL-SDDC approach.

The TLOS and VLOS of the BIEODL-SDDC method are tested on BC performance in Figure 10. The figure pointed out that the BIEODL-SDDC approach has better performance with minimal values of TLOS and VLOS. Visibly, the BIEODL-SDDC technique has reduced VLOS outcomes.
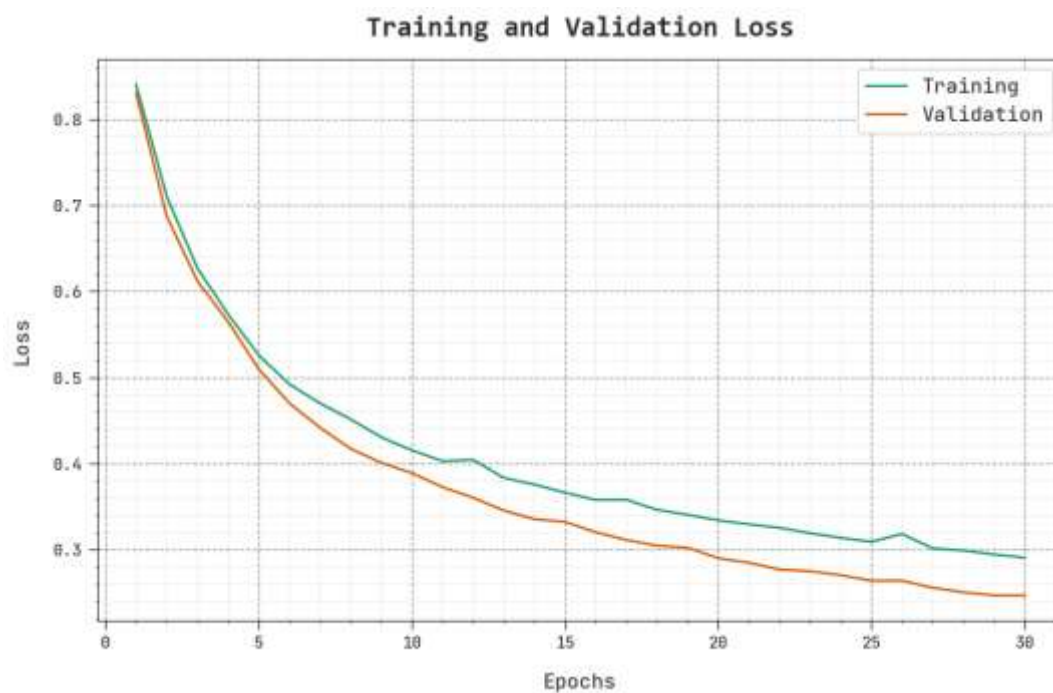
Training and Validation Loss

Figure 10. TLOS and VLOS outcomes of the BIEODL-SDDC method.

A clear precision-recall examination of the BIEODL-SDDC method under the test database is portrayed in Figure 11. The figure indicated that the BIEODL-SDDC system has enhanced values of precision-recall values under all classes.
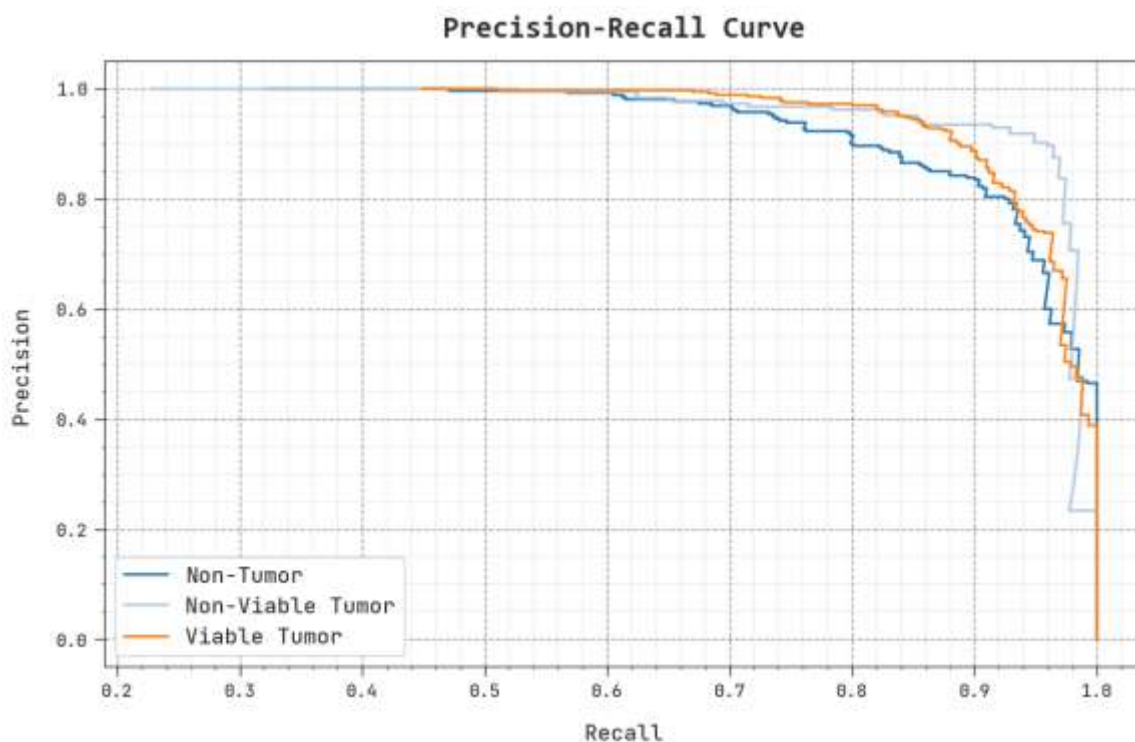
Precision-Recall Curve

Figure 11. Precision-recall outcome of BIEODL-SDDC approach.

The detailed ROC study of the BIEODL-SDDC technique under the test database is portrayed in Figure 12. The figure shows that the BIEODL-SDDC method has exposed its ability to categorize distinct classes.
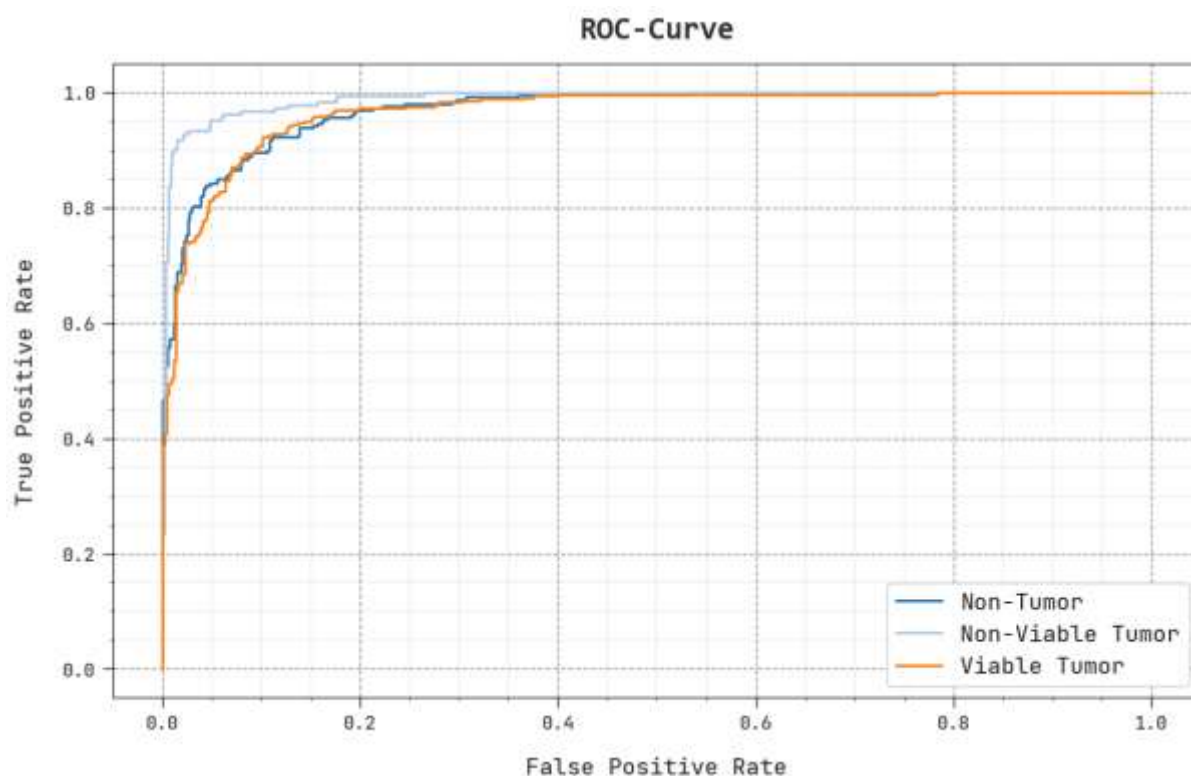

Figure 12. ROC outcome of the BIEODL-SDDC approach.

A comparison results of the BIEODL-SDDC technique with other DL models is made in Table 7 [28,29]. Figure 13 signifies the comparative outcomes of the BIEODL-SDDC method in terms of $accu_y$. The outcomes exhibit that the BIEODL-SDDC technique reaches improving values of $accu_y$. Based on $accu_y$, the BIEODL-SDDC technique gains a higher $accu_y$ of 94.81%, while the Handcrafted Feature, EfficientNet-B0, Xception, EfficientNet-B0-Handcrafted, and Xception-Handcrafted methods obtain reduced $accu_y$ of 91.90%, 89.45%, 93.16%, 90.38%, and 93.09%, respectively.

Table 7. Comparative outcome of BIEODL-SDDC approach with other DL techniques.

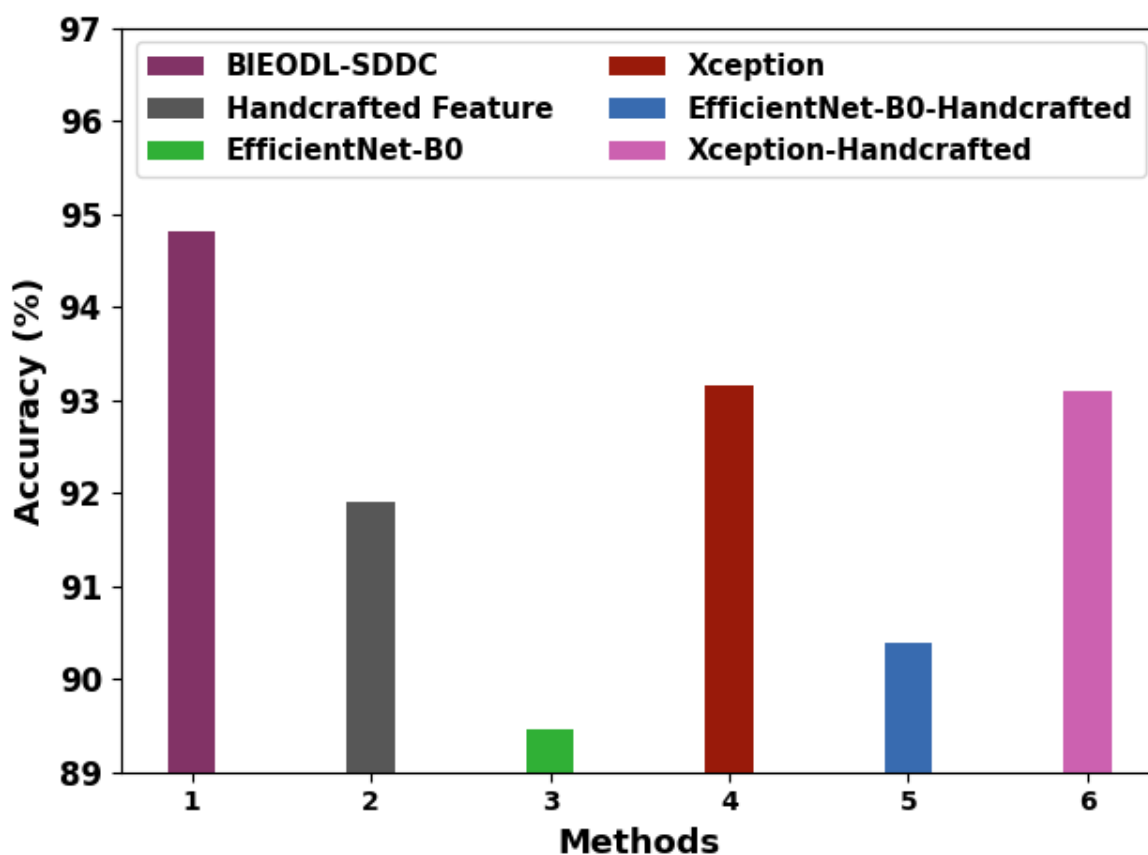| Methods	Accuracy	Precision	Recall	F-Score
BIEODL-SDDC	94.81	93.21	90.99	91.98
Handcrafted Feature	91.90	92.69	86.77	90.84
EfficientNet-B0	89.45	90.51	87.69	89.43
Xception	93.16	91.51	86.13	90.10
EfficientNet-B0-Handcrafted	90.38	90.08	88.71	89.75
Xception-Handcrafted	93.09	92.36	88.72	90.47

Figure 13. $Accu_y$ outcome of BIEODL-SDDC approach with other DL techniques.

Figure 14 demonstrates the detailed results of the BIEODL-SDDC approach in terms of $prec_n$, $reca_l$, and F_{score}. The outcomes specify that the BIEODL-SDDC approach reaches improving values of $prec_n$, $reca_l$, and F_{score}. Based on $prec_n$, the BIEODL-SDDC technique gains a higher $prec_n$ of 93.21% while the Handcrafted Feature, EfficientNet-B0, Xception, EfficientNet-B0-Handcrafted, and Xception-Handcrafted methods obtain reduced $prec_n$ of 92.69%, 90.51%, 91.51%, 90.08%, and 92.36%, respectively. Also, based on $reca_l$, the BIEODL-SDDC technique gains a higher $reca_l$ of 90.99% while the Handcrafted Feature, EfficientNet-B0, Xception, EfficientNet-B0-Handcrafted, and Xception-Handcrafted approaches obtain a reduced $reca_l$ of 86.77%, 87.69%, 86.13%, 88.71%, and 88.72% respectively.

At last, based on F_{score}, the BIEODL-SDDC technique gains a higher F_{score} of 91.98% while the Handcrafted Feature, EfficientNet-B0, Xception, EfficientNet-B0-Handcrafted, and Xception-Handcrafted approaches obtain reduced F_{score} of 90.84%, 89.43%, 90.10%, 89.75%, and 90.47%, respectively. These results pointed out that the BIEODL-SDDC technique accomplishes enhanced performance in the healthcare sector.
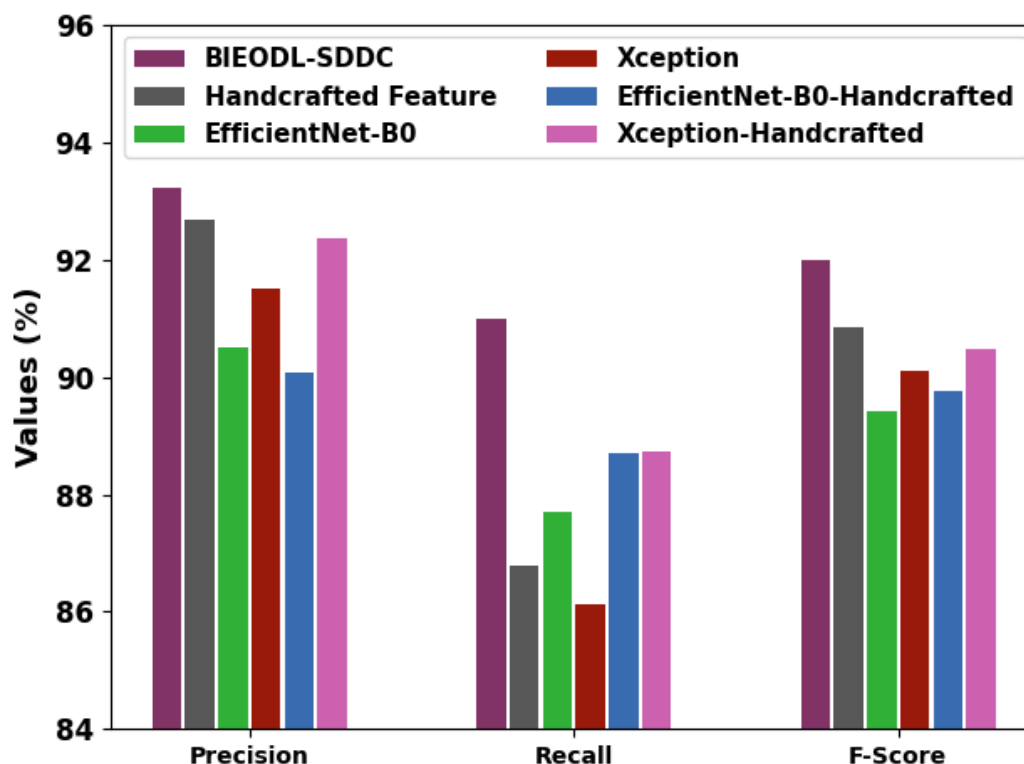
Figure 14. Comparative outcome of BIEODL-SDDC approach with other DL techniques.

5. Conclusions

In this study, a BIEODL-SDDC approach is developed for a secure and smart healthcare environment. The presented BIEODL-SDDC technique allows the secure sharing of medical images via encryption and BC technology with a DL-based disease classification process. In the presented BIEODL-SDDC technique, the medical image encryption process is performed by the GKO with the ElGamal Encryption technique. Moreover, BC-based SCs can be utilized for securely sharing medical images. For the disease detection process, the BIEODL-SDDC technique encompasses EfficientNet-B7-CBAM-based feature extraction, Adam optimizer, and FCNN. The simulation values of the BIEODL-SDDC method are tested on a medical image dataset and the outcomes proved the enhanced performance of the BIEODL-SDDC method over other existing techniques. The limitations of the BIEODL-SDDC technique include scalability with larger datasets, privacy improvement, robustness against adversarial outbreaks, generalization across medical image modalities, and regulatory compliance. Future studies may be on scalability analysis, enhancing privacy and robustness, generalization analysis, and addressing regulatory compliance.

Acknowledgment

Conflict of interest

The authors declare that they have no conflicts of interest. The manuscript was written through contributions of all authors. All authors have given approval to the final version of the manuscript.

Author contributions

F.S.A. and L.A.: Conceptualization; F.S.A.: Methodology; M.R.: Software; F.S.A. and A.M.: Validation; L.A.: Investigation; F.S.A.: Data curation; L.M., A.M. and M.R.: Writing—original draft; F.S.A., L.M., A.M. and M.R.: Writing—review & editing; A.M.: Visualization; M.R.: Project administration; F.S.A.: Funding acquisition. All authors have read and agreed to the published version of the manuscript.

Use of AI tools declaration

The authors declare they have not used Artificial Intelligence (AI) tools in the creation of this article.

References

1. P. K. Ghosh, A. Chakraborty, M. Hasan, K. Rashid, A. H. Siddique, Blockchain application in healthcare systems: A Review, *Systems*, **11** (2023), 38. https://doi.org/10.3390/systems11010038
2. S. Sai, V. Chamola, K. K. R. Choo, B. Sikdar, J. J. Rodrigues, Confluence of Blockchain and Artificial Intelligence Technologies for Secure and Scalable Healthcare Solutions: A Review, *IEEE Internet Things*, **10** (2022), 5873–5897. https://doi.org/10.1109/JIOT.2022.3232793
3. A. I. Taloba, A. Elhadad, A. Rayan, R. M. Abd El-Aziz, M. Salem, A. A. Alzahrani, et al., A blockchain-based hybrid platform for multimedia data processing in IoT-Healthcare, *Alex. Eng. J.*, **65** (2023), 263–274. https://doi.org/10.1016/j.aej.2022.09.031
4. V. Merlo, G. Pio, F. Giusto, M. Bilancia, On the exploitation of the blockchain technology in the healthcare sector: A systematic review, *Expert Syst. Appl.*, **213** (2022), 118897. https://doi.org/10.1016/j.aej.2022.09.031
5. A. I. Taloba, A. Elhadad, A. Rayan, R. M. Abd El-Aziz, M. Salem, A. A. Alzahrani, et al., A blockchain-based hybrid platform for multimedia data processing in IoT-Healthcare, *Alex. Eng. J.*, **65** (2023), 263–274. https://doi.org/10.1016/j.aej.2022.09.031
6. M. Wang, H. Zhang, H. Wu, G. Li, K. Gai, Blockchain-based Secure Medical Data Management and Disease Prediction, In *Proceedings of the Fourth ACM International Symposium on Blockchain and Secure Critical Infrastructure*, (pp 71–82), 2022. https://doi.org/10.1145/3494106.3528678
7. B. A. Dedeturk, A. Soran, B. Bakir-Gungor, Blockchain for genomics and healthcare: A literature review, current status, classification and open issues, *PeerJ*, **9** (2021), e12130. https://doi.org/10.7717/peerj.12130
8. S. Ramzan, A. Aqdus, V. Ravi, D. Koundal, R. Amin, M. A. Al Ghamdi, Healthcare applications using blockchain technology: Motivations and challenges, *IEEE Transactions on Engineering Management*, **70** (2022), 2874–2890. https://doi.org/10.1109/TEM.2022.3189734

9. P. Tagde, S. Tagde, T. Bhattacharya, P. Tagde, H. Chopra, R. Akter, et al., Blockchain and artificial intelligence technology in e-Health, *Environ. Sci. Pollut. R.*, **28** (2021), 52810–52831. https://doi.org/10.1007/s11356-021-16223-0

10. R. Shinde, S. Patil, K. Kotecha, V. Potdar, G. Selvachandran, A. Abraham, Securing AI-based Healthcare Systems using Blockchain Technology: A State-of-the-Art Systematic Literature Review and Future Research Directions, 2022, arXiv preprint arXiv:2206.04793. https://doi.org/10.1002/ett.4884

11. A. Goel, S. Neduncheliyan, An intelligent blockchain strategy for decentralised healthcare framework, *Peer Peer Netw. Appl.*, **16** (2023), 846–857. https://doi.org/10.1007/s12083-022-01429-x

12. D. Jadav, N. K. Jadav, R. Gupta, S. Tanwar, O. Alfarraj, A. Tolba, et al., A trustworthy healthcare management framework using amalgamation of AI and blockchain network, *Mathematics*, **11** (2023), 637. https://doi.org/10.1007/s12083-022-01429-x

13. I. V. Pustokhina, D. A. Pustokhin, K. Shankar, Blockchain-based secure data sharing scheme using image steganography and encryption techniques for telemedicine applications, In *Wearable Telemedicine Technology for the Healthcare Industry*, (pp. 97–108). Academic Press, 2022. https://doi.org/10.1007/s12083-022-01429-x

14. Y. Wu, L. Zhang, S. Berretti, S. Wan, Medical image encryption by content-aware dna computing for secure healthcare, *IEEE T. Ind, Inform.*, **19** (2022), 2089–2098. https://doi.org/10.1109/TII.2022.3194590

15. A. A. Noman, M. Rahaman, T. H. Pranto, R. M. Rahman, Blockchain for medical collaboration: A federated learning-based approach for multi-class respiratory disease classification, *Healthcare Analytics*, **3** (2023), 100135. https://doi.org/10.1016/j.health.2023.100135

16. B. Ren, L. T. Yang, Q. Zhang, J. Feng, X. Nie, Blockchain-Powered Tensor Meta-Learning-Driven Intelligent Healthcare System with IoT Assistance, *IEEE T. Netw. Sci. Eng.*, **10** (2022), 2503–2513. https://doi.org/10.1016/j.health.2023.100135

17. P. D. Singh, R. Kaur, G. Dhiman, G. R. Bojja, BOSS: A new QoS aware blockchain assisted framework for secure and smart healthcare as a service, *Expert Syst.*, **40** (2023), e12838. https://doi.org/10.1111/exsy.12838

18. A. Ala, V. Simic, D. Pamucar, N. Bacanin, Enhancing patient information performance in internet of things-based smart healthcare system: Hybrid artificial intelligence and optimization approaches, *Eng. Appl. Artif. Intell.*, **131** (2024), 107889. https://doi.org/10.1016/j.engappai.2024.107889

19. A. Ala, A. H. Sadeghi, M. Deveci, D. Pamucar, Improving smart deals system to secure human-centric consumer applications: Internet of things and Markov logic network approaches, *Electron. Commer. Res.*, 2023, 1–27.

20. A. Ala, V. Simic, D. Pamucar, E. B. Tirkolaee, Appointment scheduling problem under fairness policy in healthcare services: Fuzzy ant lion optimizer, *Expert Syst. Appl.*, **207** (2022), 117949. https://doi.org/10.1016/j.engappai.2024.107889

21. F. S. Alrayes, S. S. Alotaibi, K. A. Alissa, M. Maashi, A. Alhogail, N. Alotaibi, et al., Artificial intelligence-based secure communication and classification for Drone-Enabled emergency monitoring systems, *Drones*, **6** (2022), 222. https://doi.org/10.1016/j.engappai.2024.107889

22. A. Behura, M. Srinivas, M. R. Kabat, Giraffe kicking optimization algorithm provides efficient routing mechanism in the field of vehicular ad hoc networks, *J. Amb. Intel. Hum. Comp.*, **13** (2022), 3989–4008. https://doi.org/10.1016/j.engappai.2024.107889

23. R. Kumar, W. Wang, J. Kumar, T. Yang, A. Khan, W. Ali, et al., An integration of blockchain and AI for secure data sharing and detection of CT images for the hospitals, *Comput. Med. Imag. Grap.*, **87** (2021), 101812. https://doi.org/10.1016/j.engappai.2024.107889

24. X. Du, L. Si, X. Jin, P. Li, Z. Yun, K. Gao, Classification of plug seedling quality by improved convolutional neural network with an attention mechanism, *Front. Plant Sci.*, **13** (2022). https://doi.org/10.1016/j.engappai.2024.107889

25. A. Kumar, S. Sarkar, C. Pradhan, Malaria disease detection using cnn technique with sgd, rmsprop and adam optimizers, In *Deep learning techniques for biomedical and health informatics*, (pp. 211–230), Springer, Cham, 2020. https://doi.org/10.1007/978-3-030-33966-1_11

26. J. Lee, J. Kim, I. Kim, K. Han, Cyber threat detection based on artificial neural networks using event profiles, *IEEE Access*, **7** (2019), 165607–165626. https://doi.org/10.1007/978-3-030-33966-1_11

27. P. Leavey, A. Sengupta, D. Rakheja, O. Daescu, H. B. Arunachalam, R. Mishra, Osteosarcoma data from UT Southwestern/UT Dallas for Viable and Necrotic Tumor Assessment [Data set], Cancer Imaging Arch, 2019, 14.

28. T. Veeramakali, R. Siva, B. Sivakumar, P. C. Senthil Mahesh, N. Krishnaraj, An intelligent internet of things-based secure healthcare framework using blockchain technology with an optimal deep learning model, *The Journal of Supercomputing*, 2021, 1–21. https://doi.org/10.1007/978-3-030-33966-1_11

29. B. Fakieh, A. S. A. M. AL-Ghamdi, M. Ragab, Optimal deep stacked sparse autoencoder based osteosarcoma detection and classification model, *Healthcare*, **10** (2022), 1040. https://doi.org/10.3390/ healthcare10061040